# Control of Wake-Induced Exposure Using an Interrupted Oscillating Jet

**AUTHORS**
**James S. Bennett**[a]
**Keith G. Crouch**[a]
**Stanley A. Shulman**[b]

[a]Engineering and Physical Hazards Branch, MS R5, Division of Applied Research and Technology, National Institute for Occupational Safety and Health, 4676 Columbia Parkway, Cincinnati, OH 45226; [b]Monitoring Research and Statistics Activity, MS R35, Division of Applied Research and Technology, National Institute for Occupational Safety and Health, 4676 Columbia Parkway, Cincinnati, OH 45226

A problem may arise in ventilation design when the contaminant source is located in the worker's wake, where turbulence and vortex formation can carry the contaminant into the breathing zone even though the source is downwind. It was found previously that forced directional variations in the flow can reduce or eliminate the vortex formation that causes these local reversals. Reported here is a simple realization of this concept, in which an oscillating jet of air was directed at a mannequin in an otherwise steady flow of air. A 50th percentile male mannequin was placed in a nearly uniform flow of approximately 0.18 m/sec (36 ft/min). A low-velocity tracer gas source (isobutylene) was held in the standing mannequin's hands with the upper arms vertical and the elbows at 90°. Four ventilation scenarios were compared by concentration measurements in the breathing zone, using photoionization detectors: (A) uniform flow; (B) addition of a steady jet with initial velocity 5.1 m/sec ($1.0 \times 10^3$ ft/min) directed at the mannequin's back, parallel to the main flow; (C) making the jet oscillate to 45° on either side of the centerline with a period of 13 sec; and (D) introducing a blockage at the centerline so the oscillating jet never blew directly at the worker. At the 97.5% confidence level the interrupted oscillating jet (case D) achieved at least 99% exposure reduction compared with the uniform flow by itself (case A), at least 93% compared with the steady jet (case B), and at least 45% exposure reduction compared with the unblocked oscillating jet (case C).

**Keywords: computational fluid dynamics, ventilation design, vortex formation**

The physics of flow around the human body creates a challenge to ventilation designs aimed at reducing breathing-zone concentrations of air contaminants. From a fluid dynamics point of view this problem fits into the classical case of uniform external flow around a bluff body, such as a circular cylinder as a two-dimensional (2-D) example or a sphere as a three-dimensional (3-D) example.[1,2] A body in a flow creates a wake. This wake transports mass (such as an air contaminant) back toward the body, counter to the direction of the free-stream or main flow. If a contaminant source is located in this recirculation zone of the wake near the body, then some contaminant is transported toward the body even though the free-stream direction would tend to draw the contaminant away from the body.[3] This phenomenon occurs in many occupational settings. Examples are firing ranges, spray-painting booths, and laboratory hoods.[4–7]

The transport behavior of the wake depends on the size and shape of the body and characteristics of the freestream. Classes of wakes can be identified by approximate ranges of Reynolds number, the dimensionless ratio of inertial to viscous forces.[8] For a worker of a given size and shape in a flow with constant density and viscosity, the Reynolds number depends only on the flow velocity. The cases of a circular cylinder and a sphere in 2-D and 3-D flows, respectively, offer approximate analogies. The following discussion of these cases is drawn from Clift et al.,[2] Yih,[8] and Schlichting.[9] For a Reynolds number (Re) below approximately 10, the flow around a cylinder is laminar, with no recirculation or separation of the boundary layer. The same is true of a sphere for Re below 20. A cylinder of typical adult body width would require airflow velocities less than approximately 0.03 cm/sec (0.06 ft/min) to prevent recirculation in the wake. As Re

is increased, the flow, although still laminar, separates from the body and forms a recirculation zone in the near-wake region. Above Re≈60 for a cylinder and 130 for a sphere, the recirculation eddies or vorticies break away from the body and move downstream. As Re increases, the vortices are shed with increasing frequency and the pattern becomes more random until beyond approximately $2 \times 10^5$, at which point the periodic pattern has been replaced with fully developed turbulence. It is reported that periodicity reappears beyond $3 \times 10^6$. Returning to the body-sized (0.5 m diameter) cylinder in an airflow, a velocity of 18 cm/sec (36 ft/min) results in an Re of 6100.

Adjusting the velocity affects wake transport and, therefore, exposure, as other researchers have found.[10] The present study demonstrates an innovative velocity adjustment in the form of a directionally oscillating jet, continuing the work of Crouch on fluctuating flows in the occupational environment.[4,5] Here, time-weighted geometric mean concentration of a tracer gas in the breathing zone is reduced by disrupting the wake, thereby reducing its ability to accumulate the tracer gas.

The other important dimensionless quantity in this situation is the Strouhal number (S):

$$S = \frac{fD}{U} \quad (1)$$

where f is the frequency of vortex shedding from one side of the body, D is a characteristic length such as diameter, and U is the freestream velocity. Schlichting gives S as 0.21 for $500 < Re < 7000$.[9] George, Flynn, and Goodman report that S is almost always equal to about 0.21 in occupational environments.[3] With S nearly constant, the definition shows that vortices are shed more frequently as U increases.

## METHODS

### Experiment

The experimental setup consisted of a room with nearly plug flow, 0.18 m/sec (36 ft/min), incident at the back of a 50th percentile male mannequin. The room was 5.1 m long, 3.6 m wide, and 2.5 m high. A round jet created by a tabletop fan on a pedestal with initial velocity of 5.1 m/sec ($1.0 \times 10^3$ ft/min), incident at the back of the mannequin could also oscillate through a 90° angle horizontally. The jet origin was at a height of 1.2 m, and some trials involved an obstacle placed between the fan and the mannequin that was 0.25 m (10.0 inches) wide and 0.025 m (1.0 inch) thick, and reached from the floor to 1.8 m, the height of the mannequin. The setup is shown in Figure 1, with centerline distances between the supply wall, jet origin, obstacle, mannequin, tracer source, and exhaust wall shown along the bottom of the figure. Observation of flow patterns using theatrical smoke created intuition about jet and wake behavior and smoke transport. From these observations four scenarios covering a range of behavior were selected to systematically evaluate the effectiveness of the system. These were no jet, plug flow only (case A); steady jet incident at back of body (case B); jet oscillating through 90° (case C); and jet oscillating through 90°, interrupted by an obstacle at center of swing (case D). The tracer gas, isobutylene, was released from a 0.25-inch inner diameter Tygon® tube held by the mannequin's hands. Isobutylene concentration and fresh air supply were measured in the breathing zone by photoionization detectors at a frequency of 10 Hz to form 1-sec averages (N = 10) stored in a PC. Each run lasted 20 min, resulting in 1200 one-second

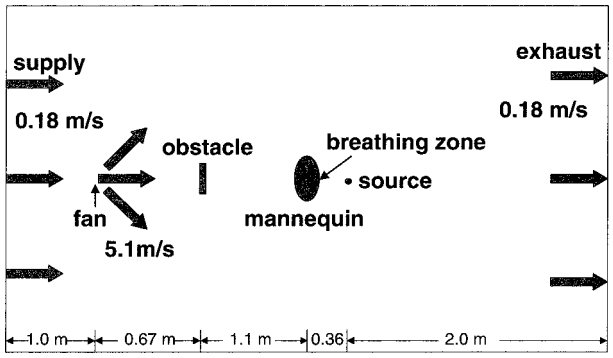


**FIGURE 1. Experimental layout and CFD geometry viewed from top of room**

averages. To ensure that a run was not affected by the previous run, the room was purged for several minutes between runs. Also, only the data from the last 15 min or 900 sec of each 20-min trial were used in calculations, to avoid the start-up period when the fluctuating concentration was clearly nonstationary. The estimates based on the last 900 sec were compared with those based on the last 600 sec and the last 300 sec. The results for these three durations differed little, and the 900-sec results are presented. For each trial a geometric mean was formed from the natural log of the 900 one-second averages. The standard deviation (SD) for each case was estimated by computing the sample SD for the 900 one-second averages. Absolute rather than geometric SD (GSD) was used as an indication of concentration variability because the GSD is related to the relative SD (RSD). The RSD is a measure of variability relative to the mean, whereas the focus of this project was variability relative to some absolute criteria, such as a ceiling limit. Also, the SD calculated here is not a direct estimate of the SD for each of the 900 averages, as these averages are autocorrelated. Still, this method provides a useful measure of concentration variability. The 15-min geometric means of breathing-zone concentrations were the primary basis for comparing the performance of the four ventilation methods, with reduction of short-term and daily exposure as motivation. The SD was used to evaluate the methods with respect to the secondary criterion of reduction of peak exposures.

The case involving the interrupted oscillating jet (case D) was evaluated according to its improvement over the other conditions—plug flow (case A), steady jet (case B), and oscillating jet (case C)—in an analysis of variance multiple comparison test. The experimental design was a block-structured factorial experiment with 4 blocks of 6 trials, 24 trials in all, with ventilation scenario randomized. All trials in a block were run on the same day. Six trials were used instead of 4 because the two oscillating jet scenarios (cases C and D) were repeated in each block to increase statistical power for the comparison of C with D. The analysis estimated the reduction in concentration of the interrupted oscillating jet (case D), relative to the other three cases. The estimated reduction was computed by taking the difference between the mean of the case of interest (A, B, or C) and the mean of D, exponentiating to obtain the ratio of the case mean to the case D mean, and subtracting the ratio from unity to obtain the fraction reduction relative to case D, as shown:

$$\%R = 100[1 - \exp(\overline{\ln C_D} - \overline{\ln C_X})]$$
$$= 100\left[1 - \frac{\exp(\overline{\ln C_D})}{\exp(\overline{\ln C_X})}\right] \quad (2)$$

where the overbars indicate means and X represents A, B, or C.

The MiniRAE 2000 PGM 7600 photoionization detectors (RAE Systems Inc., Sunnyvale, Calif.) were calibrated before and after each day of trials. The response to 100 ppm span gas was consistent to within 1%. The zero reading varied by up to 0.2 ppm. One photoionization detector (PID) measured the background concentration (consistently negligible) and was set to a range of 0–20 ppm. The other PID measured the "breathing zone" of the mannequin and was programmed for a range of 0–200 ppm. The 10.6 eV lamp was used in each trial. The analog outputs from the PIDs were processed in real-time by a DAS 1800HC analog to digital converter (Keithley Instruments Inc., Taunton, Mass.). The digital signals were processed in real-time and stored by a personal computer with a 90 MHz Pentium® processor running Labtech 10 (Laboratory Technologies Corp., Wilmington, Mass.). Air velocity was measured with a calibrated Velocicalc Plus 8386 hot-wire anemometer (TSI Inc., St. Paul, Minn.).

## Computational Fluid Dynamics (CFD)

The laboratory experiment was simulated using CFD. In a 2-D approximation of the experimental layout, the conservation equations describing fluid flow were solved numerically using the mesh-generator, Gambit 1.2, and the solver, Fluent 5.3 (Fluent, Inc., Lebanon, N.H.). Fluent utilizes the control volume approach, which involves division of the physical space into discrete control volumes called cells. The partial differential equations that govern conservation of mass, momentum, and scalar variables such as concentration are integrated over each control volume to form simplified algebraic equations. The algebraic equations are then solved iteratively, starting at the boundaries of the physical space. The calculations are repeated until the conservation laws are satisfied to an acceptable degree in each cell. The degree of imbalance, called a "residual," in the conservation law is computed as the difference between the value of a variable in a cell and the value that would be expected based on what is flowing into and out of that cell via adjacent cells. A global measure of the imbalance in the conservation law is formed by summing the residuals for all cells, then dividing by the sum of the variable in all the cells. This quantity is termed a "normalized residual."

The 2-D simulation of the experiment corresponds approximately to Figure 1. In an unstructured mesh of 46,913 hexagonal cells, the mannequin was modeled as an ellipse with minor and major axes equal to the chest depth of 20 cm (8.0 inches) and shoulder width of 46 cm (18 inches), respectively. Cell size (edge length) ranged from 0.245 cm in the boundary layer of the mannequin to 3.82 cm in the chamber freestream. Time-dependent breathing zone concentration was stored in a file as the solution progressed through time steps of 0.1 sec. At each step the solution converged so that the normalized residuals of the conservation equations were less than 0.001.

An accurate simulation requires that the cell size is small compared to important spatial elements of the flow, such as eddies, and that the time-step is brief compared to the important time-dependent behaviors, such as the separation of a vortex and its movement downstream. These resolutions are easier to achieve for low Re flows than for high, because as Re increases, smaller eddies form and flows fluctuate more rapidly. Capturing these behaviors directly (known as direct numerical simulation, or DNS) is usually too computationally expensive. An alternative is to model the turbulence in terms of the scalar variables k and $\epsilon$, the kinetic energy of turbulence and the eddy dissipation rate, respectively, and to solve conservation equations for them. The k-$\epsilon$ model has been widely used with a great deal of success for many applications. Exhaustive experiments were performed by Launder and Spalding to arrive at empirical constants that provide closure to this turbulence model.[11] Room airflows, though, are one of the applications that challenge this method. This model can be overly diffusive, and researchers have found that perturbations must be introduced to initiate vortex shedding.[12–14] Braza et al. and Dunnett successfully used the k-$\epsilon$ model in this manner for 2-D flows around a circle and an ellipse, respectively. As an alternative to the computational expense of direct simulation and the complexity involved in successful application of the k-$\epsilon$ model, the current authors chose to use an approach called large eddy simulation (LES), in which the dynamics of the larger eddies that contained most of the turbulent kinetic energy was directly simulated and the effect of the smaller eddies was modeled. The need to rely on empirical constants was thus reduced. The mesh resolution was sufficient to use the LES technique, without being overly fine and increasing numerical error. Wilcox recommends that the cell size be much smaller than flow-scale eddies and much larger than the Taylor scale, $\lambda$, where

$$\lambda \cong \left(\frac{10\nu k}{\epsilon}\right)^{1/2} \quad (3)$$

with kinetic energy of turbulence k, eddy dissipation rate $\epsilon$, and kinematic viscosity, $\nu$.[15] The suggested time step, $\tau$, is on the order of

$$\tau \cong \frac{\lambda}{U} \quad (4)$$

These criteria were satisfied at all mesh locations and at all times. Some work also was done with the k-$\epsilon$ turbulence model and with no turbulence model, for comparison with the LES results.

The oscillating jet was treated as a time-varying momentum source, for which the Fluent code was modified by a user-defined function (UDF), a program written in the C programming language that runs alongside the Fluent code, also written in C. To create the momentum source, the velocity in the cells that simulated the fan was governed by the following equations, which describe the oscillation of the fan jet:

$$U_X = \sqrt{2}A + \left|(A - \sqrt{A})\cos\left(\frac{2\pi t}{T}\right)\right| \quad (5)$$

$$U_Y = \sqrt{2}A \sin\left(\frac{2\pi t}{T}\right) \quad (6)$$

where $U_X$ and $U_Y$ are the x and y velocity components, A is the fan speed of 5.1 m/sec, t is time, and T is the fan period of 13 sec.

The point source in the 2-D simulation corresponded to a line source in 3-D space, rather than a point source in 3-D space, as in the experiment. The experimental source and the simulated source could not be geometrically similar, so the tracer gas emission rate in the simulation was arbitrarily chosen, and no attempt was made to match the absolute concentrations in the simulation with those of the experiment. This did not detract from the quality of the CFD solution, because the relationship between cases A, B,

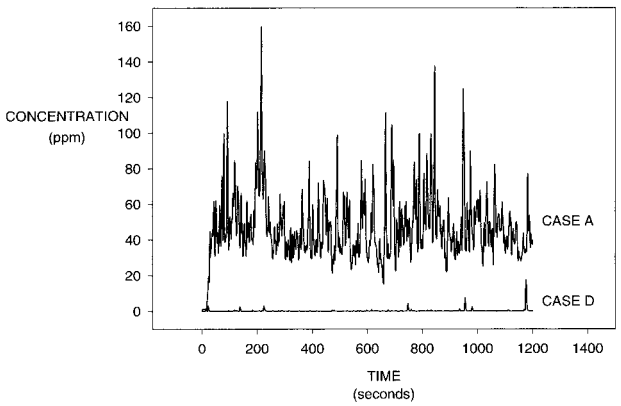


**FIGURE 2. One-second average concentration for case A: uniform flow, no jet; and for case D: interrupted oscillating jet**

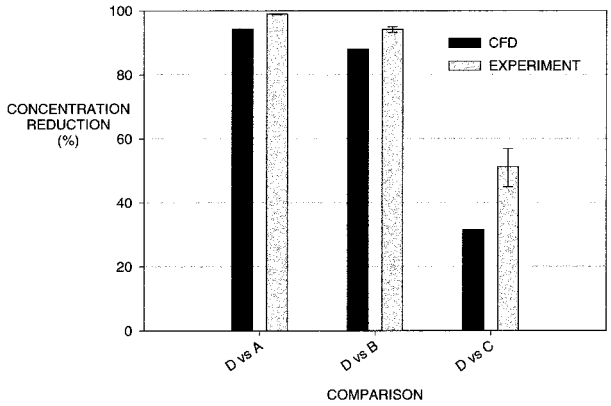


**FIGURE 3. Experimental and numerical (CFD) concentration reduction for case D relative to other cases. Simultaneous 95% confidence limits are shown for the experiment.**

C, and D (i.e., the relative concentrations) was the issue in this work. Because the CFD solutions are deterministic, only one trial was performed for each set of conditions, and Equation 3 was modified for application to the simulation results by removing the overbars, which indicate averaging, and the log and exponential functions, which are inverses of each other:

$$\%R = 100\left(1 - \frac{C_D}{C_X}\right) \quad (7)$$

## RESULTS

### Experiment

Because of large differences in magnitude among the four cases, the 900 measurements in each trial were converted to the natural log scale before averaging. The statistical analysis was based on these 24 averages. One further complication was that the measurement and datalogging system had some zero drift, resulting in many of the 1-sec averages being slightly less than zero, when the tracer gas concentration was essentially zero. About 80% of these occurrences were from case D and 20% from case C, the two cases with the lowest concentrations. The minimum value was approximately −0.26 ppm. Before converting to the natural log scale, 0.3 was added to each 1-sec average. This was equivalent to adjusting the zero of the measurement system. Adding a positive number to all the data brought the means closer together in proportionality. The estimated reductions for case D were then smaller, making the reporting of the results more conservative. The residuals from the statistical analysis are acceptable, so the authors present the estimates based on adding 0.3. The residuals from the analysis of variance model are approximately normally distributed with approximately constant variability. Thus, confidence intervals for the estimates produced by the model can be presented.

Figure 2 shows examples of breathing-zone concentration versus time plots for two of the ventilation scenarios. Although the uniform flow example (case A) requires plotting a large concentration range, the interrupted oscillating jet example (case D) is presented on the same plot for comparison. Case D appears flat and close to zero compared to case A; however, close inspection of case D reveals several peaks. As an indication of concentration variability, the SD in parts per million for all 1-sec averages was 15.6, 3.30, 2.15, and 0.70, for cases A, B, C, and D, respectively.

The geometric mean isobutylene concentrations in parts per million were 44.6, 7.32, 0.880, and 0.427, for cases A through D, respectively. The means were formed from all 15-min averages for each case. Cases A and B (plug flow and steady jet) each had four trials. Cases C and D (oscillating jet and interrupted oscillating jet) were each measured eight times. The two-sided simultaneous 95% confidence limits were (39.2, 50.6), (6.44, 8.31), (0.804, 0.963), and (0.390, 0.468). The confidence limits were formed from the analysis of variance, by means of Student's t-test statistics. Because the confidence limits are far from overlapping, the result,

$$C_A > C_B > C_C > C_D \quad (8)$$

is clearly statistically significant.

The interrupted oscillating jet emerges as the most effective control in this study. To answer the question of how much more effective this case is compared to the other three, Figure 3 displays the results of the multiple comparison test. Case D reduced the exposure by 99.0% compared to case A; 94.2% compared to Case B; and 51.3% compared to Case C. To report these results more conservatively using the lower 97.5% simultaneous confidence limits, the reductions were at least 98.9, 93.2, and 45.0%, compared to Cases A, B, and C, respectively. These are at 97.5% confidence because only one side of the two-sided 95% confidence limits shown in Figure 3 is being asserted.

### CFD

Figure 3 shows the experimental and numerical results side-by-side. The CFD simulation and experiment agree qualitatively because

$$C_A > C_B > C_C > C_D \quad (8)$$

for both. Good quantitative agreement in the relation of the four cases also was achieved, considering that the simulation was 2-D. Recall from the Methods section, however, that the tracer gas emission rate in the simulation was arbitrarily chosen. Therefore, comparing the absolute concentrations in the experiments and the simulations has no meaning. Only the reduction in concentration for case D relative to the other cases is reported here. These are

94.4, 88.0, and 31.5%, for case D compared to cases A, B, and C, respectively.

## DISCUSSION

### Experiment

Plug flow produced a fairly stable circulation pattern between the body and the tracer source. Although Re even for case A's freestream velocity of 0.18 m/sec was well into the range where vortex shedding occurs, the shedding happened slowly. Observation of the theatrical smoke under case A conditions revealed the breathing zone to be densely filled with smoke that was not dissipated effectively. The steady jet with an initial velocity of 5.1 m/sec reduced the breathing zone concentration. The factors in case B that diminished the concentration were apparently stronger than those that increased it. In other words, a combination of increased rates of clean air dilution and vortex shedding worked to lower the concentration,[3,10] but intensified turbulent diffusion probably worked to increase the breathing zone concentration, reducing the efficiency of this approach. The oscillating jet with a period of 13 sec prevented eddies from growing into coherent recirculation patterns. Vortex shedding also occurred, most noticeably during the portion of the cycle when the jet increased the velocity incident on the mannequin. Additionally, contaminated breathing zone air was entrained in the jet as it swept to the side of the mannequin, drawing it away toward the side. Other researchers have reported reduced exposure when a worker is in a side flow.[3] Blocking the jet at the center of the sweep (case D), so that it never blows directly at the worker, utilized the positive removal aspects of the jet without increasing transport into the breathing zone through turbulent diffusion. The interrupted oscillating jet still prevents eddies from growing, but forms fewer new eddies.

### CFD

The close qualitative agreement and fairly good quantitative agreement of the CFD results and the experimental results indicate that the 2-D simulation captured most of the important behavior of the system. Because the CFD results showed a less dramatic improvement going from case A through to case D, there is a 3-D effect that further improves the oscillating jet relative to the other cases. However, differences between CFD and experiment are not wholly unwelcome in this application, in that a similar trend in the CFD solution (with known departures from the experimental conditions) implies a robustness of this ventilation approach, as if it had been tested under different experimental conditions, such as a column rather than a point source and a vertical plane jet rather than a round jet. The 2-D CFD solution may have overestimated eddy stability (making them less disruptable) because eddies were limited, of course, to being 2-D. Such eddies are not subjected to stretching along or tilting of their axis of rotation, and they can exhibit self-organization.[16,17]

A 3-D simulation would have required far more computing resources with perhaps only marginally greater accuracy, because the transience of eddies was the essential behavior, here. A time-dependent treatment of turbulence, such as LES, or direct numerical simulation was, therefore, necessary.

The strengths and weaknesses of various turbulence models can be used to deconstruct the overall flow into its different aspects. To test the idea that turbulent diffusion was transporting contaminant from the source back to the breathing zone in the high velocity cases (B, C, and D), the simulations were run with no turbulence model, so that the diffusive effect of eddies smaller than the grid scale was neglected. The concentration in the breathing zone was greatly reduced. Moreover, when the simulations were run with the standard k-$\epsilon$ turbulence model, which is often overly diffusive, the concentration was much greater than that found using the LES turbulence model.[12]

## CONCLUSION

Through experiments in the ventilation laboratory and numerical simulations, up to 99.0% reduction of air contaminant exposure from a source in the near wake region was demonstrated. Diminishment of concentration variability also was shown. These controls, addressing daily, short-term, and peak exposures, were achieved through hastening eddy decay by disturbing the flow upstream of the mannequin and through minimizing eddy formation by reducing the velocity incident on the mannequin's back. The extent of agreement between experiment and CFD allows CFD to be used for future design work. Numerous designs of varying jet characteristics, such as oscillation period, can be tested numerically in 2-D and 3-D before one is chosen to be built as a prototype for testing in the laboratory and the field. This testing can in turn provide data for further validation of the CFD approach. Alternatively, the extent of approximation involved in simulating the experiment suggests that the interrupted oscillating jet method is robust, because both investigative approaches revealed similar exposure reductions.

The authors anticipate further evaluation of this approach to airborne contaminant exposure control in workplaces having a steady ventilation airflow directed at the worker's back. Also, the job should involve relatively little movement of the worker's body much of the time, and the contaminant source should be within the recirculation zone of the wake for optimal applicability of this new control method.

## REFERENCES


1. **Hinze, J.O.:** *Turbulence*. New York: McGraw-Hill, 1975. pp. 8–10.
2. **Clift, R., J.R. Grace, and M.E. Weber:** *Bubbles, Drops, and Particles*. San Diego: Academic Press, 1978. pp. 99–109.
3. **George, D.K., M.R. Flynn, and R. Goodman:** The impact of boundary layer separation on local exhaust design and worker exposure. *Appl. Occup. Environ. Hyg. 5*:501–509 (1990).
4. **Crouch, K.G., T. Peng, and D.J. Murdock:** Ventilation control of lead in indoor firing ranges: Inlet configuration and booth and fluctuating flow contributions. *Am. Ind. Hyg. Assoc. J. 52*:81–91 (1991).
5. **Crouch, K.G.:** *Variable Air Flow Eddy Control*. U.S. Patent 5,027,694. (1991).
6. **Kim, T., and M.R. Flynn:** The effect of contaminant source momentum on a worker's breathing zone concentration in a uniform freestream. *Am. Ind. Hyg. Assoc. J. 53*:757–766 (1992).
7. **Altemose, B.A., M.R. Flynn, and J. Sparkle:** Application of a tracer gas challenge with a human subject to investigate factors affecting the performance of laboratory fume hoods. *Am. Ind. Hyg. Assoc. J. 59*: 321–327 (1998).
8. **Yih, C.S.:** *Fluid Mechanics; A Concise Introduction to the Theory*. Ann Arbor: West River Press, 1977. pp. 50, 352–354.
9. **Schlichting, H.:** *Boundary-Layer Theory*. New York: McGraw-Hill, 1979. pp. 16–18, 31, 32.
10. **Gomes, M.S.P., J.H. Vincent, and D.Y.H. Pui:** The effect of freestream turbulence on the transport of particles in the vicinity of a blunt flow obstacle. *Atmos. Environ. 33*:4459–4468 (1999).

11. **Launder, B.E., and D.B. Spalding:** *Lectures in Mathematical Models of Turbulence*. London: Academic Press, 1972. pp. 74–77, 90–110.

12. **Nielsen, P.V.:** The selection of turbulence models for prediction of room airflow. *ASHRAE Trans. 104*:1119–1127 (1998).

13. **Dunnett, S.J.:** A numerical investigation into the flow field around a worker positioned by an exhaust opening. *Ann. Occup. Hyg. 38*:663–686 (1994).

14. **Braza, M., Chassaing, P., and H. Ha Minh:** Numerical study and physical analysis of the pressure and velocity fields in the near wake of a circular cylinder. *J. Fluid Mech. 165*:79–130 (1986).

15. **Wilcox, D.C.:** *Turbulence Modeling for CFD*. La Canada: DCW Industries, 2000. pp. 377–381.

16. **Tennekes, H., and J.L. Lumley:** *A First Course in Turbulence*. Cambridge, Mass.: MIT Press, 1972. pp. 2, 75–95.

17. **van Heijst, G.J.F.:** Self-organization of two-dimensional flows. *Nederlands Tijdschrift voor Natuurkunde 59*:321–325 (1993).